EarlyView publication on wileyonlinelibrary.com
(issue and page numbers not yet assigned;
citable using Digital Object Identifier – DOI)

Phys. Status Solidi A, 1–6 (2012) / DOI 10.1002/pssa.201228506

physica status solidi a
www.pss-a.com
applications and materials science

Effect of TMGa preflow on the properties of high temperature AlN layers grown on sapphire

Ronny Kirste*[,1], Markus R. Wagner[1], Christian Nenstiel[1], Frank Brunner[2], Markus Weyers[2], and Axel Hoffmann[1]

[1] TU Berlin, Institut für Festkörperphysik, Hardenbergstraße 36, 10623 Berlin, Germany
[2] Ferdinand Braun Institut, Gustav-Kirchhoff Str. 4, 12489 Berlin, Germany

Received 25 July 2012, revised 24 September 2012, accepted 1 October 2012
Published online 30 October 2012

Keywords AlN, buffer layers, exciton pressure coefficient, nitrides, photoluminescence, Raman spectroscopy

* Corresponding author: e-mail rkirste@physik.tu-berlin.de, Phone: +49-30-314-22065, Fax: +49-30-314-22064

The effect of a trimethylgallium (TMGa) preflow on the structural and optical properties of MOCVD grown AlN layers on sapphire substrates is investigated. Secondary ion mass spectroscopy measurements were performed to investigate the incorporation of Ga in the layers. It is shown that for AlN layers grown with a TMGa preflow Ga atoms incorporate mainly near the substrate/epilayer interface. Photoluminescence spectra exhibit a free exciton and a donor bound exciton. By analyzing the full width at half maximum of the free exciton and the defect luminescence an increased optical quality for the sample grown with TMGa preflow is demonstrated. Additionally, Raman spectroscopy reveals a higher crystal quality for this sample. Comparing the results from Raman spectroscopy and luminescence measurements a shift rate of 60 meV GPa^{-1} is determined for the free A-exciton. Finally, cross-sectional Raman spectroscopy is used to compare the strain at the AlN/sapphire interface for a sample grown with and without TMGa preflow.

© 2012 WILEY-VCH Verlag GmbH & Co. KGaA, Weinheim

1 Introduction Due to its adjustable direct bandgap between 3.4 eV (GaN) and 6.2 eV (AlN) and its radiation and mechanical hardness the ternary AlGaN system received much attention over the last few years. Nowadays, it is already used for light emitting diodes, field effect transistors and photodetectors [1–3]. Thereby, especially for ultra violet (UV) laser devices the growth of AlGaN/GaN or AlGaN/AlN quantum well (QW) films has proven to be a good approach for efficient emission sources [4].

Normally, a typical substrate for these QWs consists of GaN or AlN layers, with some μm thickness, grown on sapphire substrates. Often GaN/sapphire is chosen due to the fact that GaN can be grown at lower temperatures than AlN and with much higher quality. On the other hand, an AlN/sapphire template might be more useful in order to decrease lattice mismatch strain, especially for AlGaN with high Al contents, and to provide UV transparency for bottom emitter devices [5]. Thus, the control and understanding of the growth mechanism of high quality AlN layers is an essential precondition for the growth of AlGaN/AlN based devices. In order to obtain an increased crystal quality and surface morphology of such layers the use of special nucleation layers and surfactants became popular. Thereby, different surfactants such as silicon and indium were tested [6, 7]. Among the surfactants used was also Ga, which could strongly reduce dislocation density and increase surface morphology for AlN layers grown on SiC [8, 9]. However, the usage of Ga during the initial growth stages on the crystal quality of thin (Al,Ga)N layers on sapphire was investigated sporadic, so far [10].

In this work, results from Raman spectroscopy, secondary ion mass spectroscopy (SIMS) and photoluminescence (PL) on AlN layers grown on a sapphire substrate with and without a short TMGa preflow at the start of the high-temperature AlN growth process are presented. The results from these measurements are compared to those from a sample grown with a longer Ga incorporation time caused by Ga residuals in the MOVPE growth chamber. Till now, little is known about the influence of such Ga supply on the properties of AlN epilayers. Within this work, it is demonstrated, that it leads to an increased crystal quality of the AlN layer, expressed by a decreased full width at half

© 2012 WILEY-VCH Verlag GmbH & Co. KGaA, Weinheim

maximum (FWHM) of the strain sensitive E_2(high) mode. This finding is confirmed by results from PL measurements showing reduced FWHM of the free excitons and decreased defect luminescence. Combining the results from Raman and luminescence measurements, a pressure coefficient for the A-exciton of AlN is determined. Finally, cross sectional Raman spectroscopy is applied to investigate the strain relieve mechanisms from the interface towards the surface.

2 Experiments To investigate the effect of a TMGa preflow, five samples of AlN were grown by high-temperature MOVPE on sapphire substrates in an AIX2400G3-HT planetary reactor. Details of the high temperature growth process have already been published and can be found elsewhere [11]. The growth temperature was 1400 °C, measured pyrometrically at the susceptor backside. For all samples, the reactor pressure during growth was 50 mbar with a TMAl flow of 200 sccm. Two samples were grown with an additionally applied TMGa flow of 10 sccm for 2 min at the start of the AlN layer growth. Additionally, one sample was grown in a reactor, which was contaminated by Ga from preceding GaN epitaxy. Table 1 gives an overview about the investigated samples. It can be seen, that the AlN layers of the samples have different thicknesses. Thereby, two sets of samples have to be distinguished: Samples A, B, and C which have a thickness around 0.7 μm and D and E which have a thickness around 1.4 μm (due to increased growth time). The last set was grown, since samples with this thickness are most interesting for cross sectional Raman measurements due to the resolution of the applied set-up [12]. Furthermore, the relationship between strain, crystal quality and layer thickness can be investigated with these samples.

The samples were investigated using SIMS, Raman spectroscopy, and PL spectroscopy. Raman spectroscopy was performed with a Dilor XY 800 triple grating spectrometer at room temperature. The excitation source was the 488 nm line of an Argon laser, the resulting signal was detected by LN_2 cooled charge-coupled device (CCD) array. On plane spectra were taken in $z(xx)\underline{z}$ backscattering geometry. For in plane measurements, i.e. $x(yy)\underline{x}$ geometry, the samples were mounted onto a copper block and turned by 90°, so that the *c*-axis of the AlN layers was perpendicular to the incident laser. For that set-up a line scan was performed with an XY-table. The step width was chosen to be 250 nm due to the spot size of the laser of around 500 nm. All spectra were calibrated with a neon light source. The PL measurements were performed using the 193 nm line of an ArF laser (repetition rate 80 Hz). Temperature dependent PL measurements in the range from 5 to 300 K were made using a constant flow cryostat from Cryovac. For the detection a 0.75 m single grating spectrometer and a bi-alkali detector were used. To avoid reflection from the laser beam the PL excitation was performed under an angle of around 60° to the *c*-axis of the AlN layer. All spectra were corrected for the system response of the PL set-up.

Table 1 Specifications of the investigated samples.

sample	AlN layer thickness (μm)	growth temperature (°C)	Ga preflow
A	0.66	1400	
B	0.62	1400	10 sccm for 2′
C	0.72	1400	residue Ga in reactor
D	1.45	1400	
E	1.37	1400	10 sccm for 2′

3 Results and discussion In order to investigate the incorporation of Ga at the AlN/sapphire interface SIMS measurements were performed. Figure 1 shows the Ga count rate as a function of sputter depth for samples A, B, C, and E. For the sample without TMGa supply at the growth start (sample A) no signal above the noise level has been detected, thus, the Ga concentration in the AlN layer is negligible. A similar observation was made for the thick sample D (not shown). For the samples with a TMGa preflow, a strong Ga signal near the substrate/layer interface is observed. The shape of the signal is nearly Gaussian and similar for both samples. The FWHM of the signal is around 120 nm, indicating an incorporation of the Ga atoms only close to the sapphire interface. Similar thicknesses were observed by Kachi et al. [13] for GaN/InN/AlN layer structures. In contrast to the samples grown with the intentional TMGa preflow, sample C exhibits a strong Ga signal not only close to the sapphire interface, but also through the whole AlN layer. Although it has a maximum at the interface similar to sample B, it steadily decreases to a minimum located around 200 nm below the surface of the AlN layer. From this minimum towards the surface of the AlN

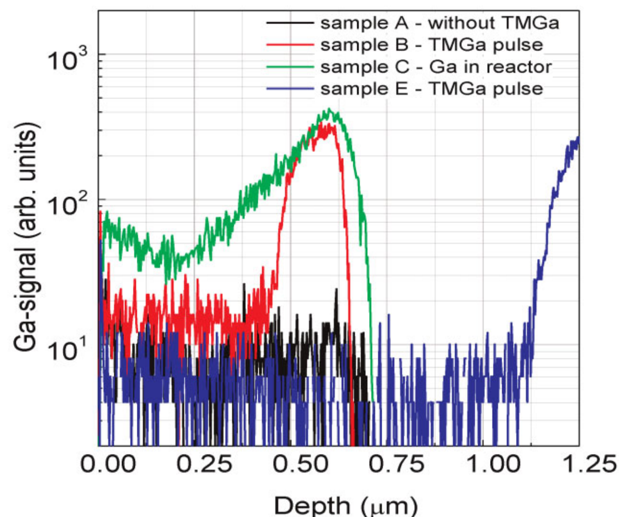

Figure 1 (online color at: www.pss-a.com) Depth profiles of the Ga count rate extracted from SIMS measurements of samples A (without TMGa), B (with TMGa preflow), C (Ga deposits in reactor), and E (with TMGa preflow).

© 2012 WILEY-VCH Verlag GmbH & Co. KGaA, Weinheim

layer, a small increase of the Ga signal can be observed. As mentioned above, this sample was grown in a Ga contaminated reactor chamber. The maximum of the Ga signal at the AlN/sapphire interface and the following decrease can be explained by a cleaning effect of the reactor due to the high AlN growth temperature. The slight increase of the signal towards the surface may be explained by a thin Ga layer segregating on the AlN layer during the growth process, which can result in a measurable Ga incorporation at the layer surface. This would be an unintentional surfactant, which was used in AlN growth before. For such a surfactant Moe and co-workers [14] reported a positive effect on the crystal quality for the growth on sapphire. Origin of this positive influence could be the fact that in this case the surface is terminated by Ga (the cation in GaN), which has proven to have an enhancing effect on the crystal quality in other hexagonal materials [15, 16].

In order to assess the optical quality of the epilayers and to get information about impurity incorporation, PL measurements were performed. Figure 2a shows low-temperature PL results from the three thinner samples A to C in the spectral range of the free A-exciton [17]. All spectra were fitted; the resulting peak positions and the associated FWHMs are listed in Table 2.

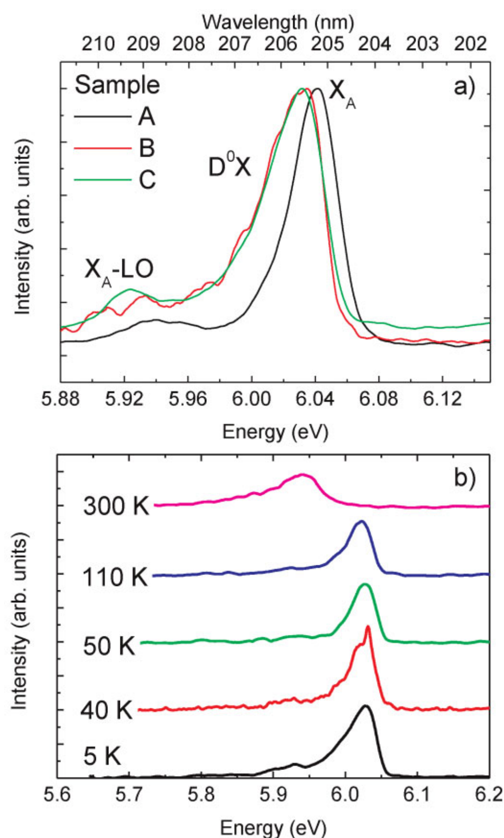

Figure 2 (online color at: www.pss-a.com) (a) Photoluminescence spectra of the three thinner AlN samples (A–C) in the range of exciton emission measured at 5 K. Peaks were normalized to the maximum for clarity. (b) Temperature dependence of the near band edge luminescence of sample B.

Table 2 Position and FWHM of the 5 K PL peaks observed in the energetic range of the free exciton.

sample	FX_A (eV)	FWHM (eV)	D^0X (eV)	FWHM (eV)	Ga
A	6.041	0.030	6.024	0.046	–
B	6.036	0.022	6.017	0.041	preflow
C	6.034	0.028	6.013	0.049	reactor

A typical PL spectrum for all samples contains a strong high-energy peak with a weaker low energy shoulder and an associated phonon replica at lower energies. The peak with the highest peak energy is identified as the free A-exciton (FX_A) of AlN using the temperature dependent measurements displayed in Fig. 2b. This identification is easily made taking into account the intensity behavior of this peak and especially the fact that it is still observable at room temperature. The low energy flank is identified as a donor bound exciton (D^0X) related to silicon [18]. Its intensity decreases much faster so that it is not observable for temperatures above 50 K. The intensity ratio FX_A/D^0X at low temperatures is very unusual as the bound exciton should dominate the spectrum due to its binding energy, which is above the thermal energy [19, 20]. However, such behavior was observed before [21, 22] and might be explained by band filling effects due to the pulsed excitation or simply a low donor concentration. For sample A, the energetic position of the free exciton is 4 meV above values typically published for the FX_A, and for all other samples in the range of these values [20–22]. It should be mentioned that, although the authors do not mention it explicitly, their samples are probably unstrained since especially the results on AlN published by Feneberg et al. [22] were for layers grown on bulk AlN. However, a correlation of X-ray diffraction, Raman spectroscopy and luminescence measurements by Prinz et al. demonstrated that tensile strain can lead to a shift of the exciton to lower energies [23]. Thus, a possible explanation for the discrepancy between the position of the FX_A between sample A and the results published by Prinz and Feneberger could be a small compressive strain in the layer. However, this cannot be confirmed by Raman spectroscopy measurements (Fig. 3). Thereby, it is seen that sample A is nearly strain free so that strain cannot lead to the PL offset. Furthermore, band-filling effects due to high excitation density can also be excluded, since power dependent measurements with excitation power densities up to 40 MW cm^{-2} did not reveal a shift of the free A exciton [22]. Following this argumentation, the origin of the shift of the FX_A transitions in sample A cannot be conclusively determined, only strain and band filling effects can be excluded.

The shift of the FX_A peak to lower energies for sample B and C compared to sample A is explained by tensile strain in these layers. This is confirmed by Raman spectroscopy and

 © 2012 WILEY-VCH Verlag GmbH & Co. KGaA, Weinheim

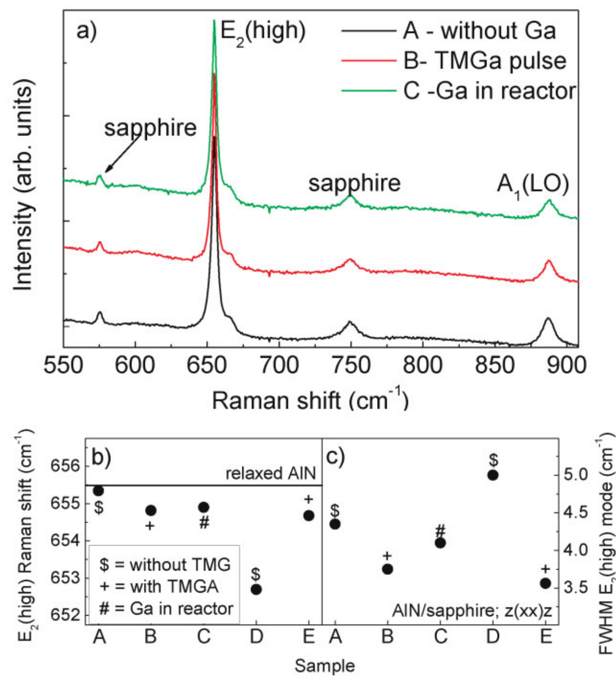

Figure 3 (online color at: www.pss-a.com) (a) Typical Raman spectra of the three thin samples (A–C). Position (b) and full width at half maximum (FWHM) (c) of the strain sensitive E_2(high) mode of AlN. Samples without Ga incorporation are marked with a dollar sign, samples with TMGa preflow are marked with a plus sign, and the sample grown in a Ga contaminated reactor is marked with a hash sign.

will be discussed below. One could argue that the incorporation of Ga into the AlN layers could lead to an AlGaN like behavior, which would lead to a shift of the free exciton transition and the Raman modes as well. But, taking into account results from SIMS measurements, one can see that sample B has no Ga incorporated close to the surface, which is identified as the main luminescence emission area. Thus, the origin of the shift of the free exciton transition must be strain, probably introduced by Ga at the substrate to layer interface. It should be mentioned that the FWHM of the free A-exciton is lowest in the sample with TMGa flow at the growth start (B), this sample has the highest optical quality, followed by the sample grown with Ga deposits in the reactor. Consequently, the initial incorporation of Ga leads to an improved optical quality accompanied by increased tensile strain.

Additionally to the excitons, two broad peaks around 3.1 and 4.3 eV can be seen in all samples (not shown). They are attributed to oxygen related impurities and nitrogen vacancies, respectively [24]. It shall be mentioned that the intensity ratio between the exciton and the defect related luminescence is around 2:1 for samples A and C and around 6:1 for sample B, indicating decreased defect incorporation and increased optical quality for the sample grown with the Ga preflow.

On plane, Raman spectra from all five samples were taken in $z(xx)\underline{z}$ backscattering geometry and spectra of the three thinner samples are displayed in Fig. 3a. In this geometry, the E_2(low), E_2(high) and the A_1(LO) mode are allowed for wurtzite AlN. Indeed, all three modes can be observed. In addition, the E_1(TO) appears at around $558\,\mathrm{cm}^{-1}$, probably due to disorder activation. Except for typical Raman modes of sapphire no other additional lines, whether AlN or defect related can be observed. Based on the appearance of the different Raman modes, no differences are noticeable between the five samples. However, a variation can be seen for the position and the FWHM of the E_2(high) mode. This is illustrated in Fig. 3b and c. The non-polar E_2(high) mode is only affected by strain, not by electric fields in the sample. Thus, it is a good indicator for strain fields. The relaxed value of the E_2(high) mode is $655.5\,\mathrm{cm}^{-1}$ [25]. As shown in Fig. 3b, except for sample A, all samples exhibit at least a small tensile strain which is maximal for the thickest sample D. This tensile strain is approved by the increasing concave wafer bow during growth, as observed by *in situ* curvature measurements.

Taking results from pressure dependent Raman spectroscopy into account, the strain related pressure within the layers can be directly calculated [25]. One can compare the Raman shift and the shift of the free exciton and estimate the strain induced shift of the FX_A, using the pressure coefficient of the E_2(high) mode of AlN ($\delta\omega/\delta p = 4.99\,\mathrm{cm}^{-1}\,\mathrm{GPa}^{-1}$). This leads to a strain induced shift of around $60\,\mathrm{meV\,GPa}^{-1}$ for the FX_A transition. This value is comparable to typical values in GaN [26]. As mentioned, the Raman shift of the E_2(high) mode of sample D is with a value of $652.5\,\mathrm{cm}^{-1}$ the smallest of all samples investigated, leading to a calculated strain of 0.6 GPa for this sample. By contrast sample E, which was grown with a TMGa preflow, is only slightly strained. The reason for the reduced tensile strain can either be a compensation effect of the Ga-induced lattice expansion or a change in the growth mode by adding Ga to the growing surface. As will be discussed the next section the latter explanation seems more favorable. A clear positive effect of the Ga containing buffer layer is evidenced by the FWHM of the E_2(high) mode. Normally, extended defects lead to a broadening of this mode, thus the FWHM can be interpreted as an indicator for the crystal quality of the layer. Figure 3c displays the FWHM of the E_2(high) mode. It can be seen that this value decreases for all AlN layers, independent of their thickness, if the samples were grown using an initial TMGa flow. Furthermore, even for the sample grown with the reactor contamination a smaller FWHM, i.e. a higher crystal quality compared to the sample without Ga can be achieved.

Following, cross sectional Raman spectroscopy is discussed to study the effect of the additional Ga incorporation during the AlN growth start [27]. Raman spectra were taken at different points on the cross-section of the sample.

© 2012 WILEY-VCH Verlag GmbH & Co. KGaA, Weinheim

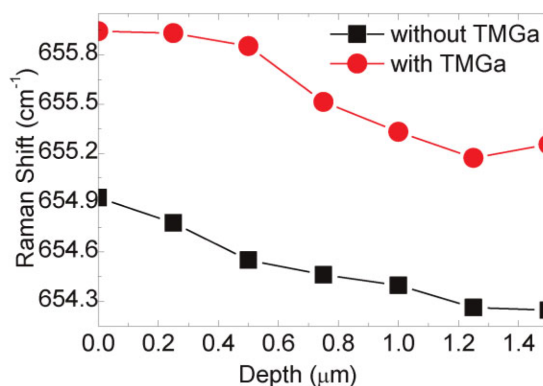

Figure 4 (online color at: www.pss-a.com) Position of the strain sensitive E_2(high) Raman mode of samples D and E as a function of depth with respect to the surface.

Considering the spot size of the laser, which can be estimated to 500 nm, measurements at points in a distance of 250 nm lead to a complete picture of the behavior of the Raman modes in that area. In the $x(yy)\underline{x}$ geometry, the non polar E_2(high) and the polar A_1(TO) modes are allowed; consequently, it is possible to gain information about strain depending on the depth in the layer. The two thick samples were chosen for this investigation (D + E). Figure 4 shows the position of the E_2(high) mode depending on the depth of the AlN layer. As mentioned above the Raman shift of the E_2(high) mode is only affected by strain in the sample. Similar to the on-plane measurements, the sample grown without any Ga reveals a stronger tensile strain than the sample grown with the TMGa pulse. Both samples exhibit a comparable depth dependent behavior. At the interface between layer and substrate a stronger tensile strain is observed, which relaxes towards the surface, leading to increased Raman shifts. This profile confirms that the Ga incorporation at the substrate interface is not accompanied by compressive stress as would be expected by considerable replacement of Al by Ga lattice atoms. The incorporated amount of Ga is simply too low to account for that. The deduced cross-sectional strain profile therefore reveals the effect of partial relaxation with increasing growth thickness. The difference in strain between the AlN layers with and without Ga is probably linked to a different growth mode: As discussed earlier Ga acts as a surfactant resulting in a smoother surface morphology and probably a more relaxed AlN lattice [11].

4 Conclusion In summary, we investigated MOVPE grown AlN layers of different thicknesses with and without intentional Ga incorporation by means of SIMS, PL, and Raman spectroscopy. SIMS measurements showed for the samples grown with a TMGa preflow a restricted Ga incorporation close to the AlN/sapphire interface. PL revealed an increased optical quality of these samples, expressed by a low FWHM of the free exciton transition and a decreased defect-exciton luminescence ratio. Raman measurements confirmed the positive effect of the TMGa preflow by a decreased FWHM of the E_2(high) mode.

Acknowledgements Part of the work was supported by DFG within the SFB787.

References

[1] H. Kawai, M. Hara, F. Nakamura, and S. Imanaga, Electron. Lett. **34**, 592–593 (1998).
[2] K. H. Kim, Z. Y. Fan, M. Khizar, M. L. Nakarmi, J. Y. Lin, and H. X. Jiang, Appl. Phys. Lett. **85**, 4777–4779 (2004).
[3] J. Li, Z. Y. Fan, R. Dahal, M. L. Nakarmi, J. Y. Lin, and H. X. Jiang, Appl. Phys. Lett. **89**, 213510–213513 (2006).
[4] G. Kipshidze, V. Kuryatkov, K. Zhu, B. Borisov, M. Holtz, S. Nikishin, and H. Temkin, J. Appl. Phys. **93**, 1363–1366 (2003).
[5] R. Collazo, J. Xie, B. E. Gaddy, Z. Bryan, R. Kirste, M. Hoffmann, R. Dalmau, B. Moody, Y. Kumagai, T. Nagashima, Y. Kubota, T. Kinoshita, A. Koukitu, D. L. Irving, and Z. Sitar, Appl. Phys. Lett. **100**(19), 191914–191915 (2012).
[6] V. Lebedev, F. M. Morales, H. Romanus, S. Krischok, G. Ecke, V. Cimalla, M. Himmerlich, T. Stauden, D. Cengher, and O. Ambacher, J. Appl. Phys. **98**, 093508–093506 (2005).
[7] S. Keller, S. Heikman, I. Ben-Yaacov, L. Shen, S. P. DenBaars, and U. K. Mishra, Appl. Phys. Lett. **79**, 3449–3451 (2001).
[8] K. Jeganathan, M. Shimizu, T. Ide, and H. Okumura, Phys. Status Solidi B **240**, 326 (2003).
[9] T. M. Al tahtamouni, J. Li, J. Y. Lin, and H. X. Jiang, J. Phys. D **45**, 285103 (2012).
[10] R. Gutt, L. Kirste, T. Passow, M. Kunzer, K. Köhler, and J. Wagner, Phys. Status Solidi B **247**, 1710–1712 (2010).
[11] F. Brunner, H. Protzmann, M. Heuken, A. Knauer, M. Weyers, and M. Kneissl, Phys. Status Solidi C **5**, 1799–1801 (2008).
[12] R. Kirste, R. Collazo, G. Callsen, M. R. Wagner, T. Kure, J. S. Reparaz, S. Mita, J. Xie, A. Rice, J. Tweedie, Z. Sitar, and A. Hoffmann, J. Appl. Phys. **110**(9), 093503–093509 (2011).
[13] T. Kachi, K. Tomita, K. Itoh, and H. Tadano, Appl. Phys. Lett. **72**, 704–706 (1998).
[14] Y. W. Craig, G. Moe, S. Keller, J. S. Speck, S. P. DenBaars, and D. Emerson, Phys. Status Solidi A **203**, 1708–1711 (2006).
[15] M. R. Wagner, T. P. Bartel, R. Kirste, A. Hoffmann, J. Sann, S. Lautenschlager, B. K. Meyer, and C. Kisielowski, Phys. Rev. B **79**, 035307–035307 (2009).
[16] R. Kirste, M. R. Wagner, J. H. Schulze, A. Strittmatter, R. Collazo, Z. Sitar, M. Alevli, N. Dietz, and A. Hoffmann, Phys. Status Solidi A **207**, 2351–2354 (2010).
[17] J. Li, K. B. Nam, M. L. Nakarmi, J. Y. Lin, and H. X. Jiang, Appl. Phys. Lett. **81**, 3365–3367 (2002).
[18] B. Neuschl, K. Thonke, M. Feneberg, S. Mita, J. Xie, R. Dalmau, R. Collazo, and Z. Sitar, Phys. Status Solidi B **249**(3), 511–515 (2012).
[19] M. A. Reshchikov and H. Morkoc, J. Appl. Phys. **97**, 061301–061395 (2005).
[20] K. B. Nam, J. Li, M. L. Nakarmi, J. Y. Lin, and H. X. Jiang, Appl. Phys. Lett. **82**, 1694–1696 (2003).
[21] J. Li, K. B. Nam, M. L. Nakarmi, J. Y. Lin, H. X. Jiang, P. Carrier, and S.-H. Wei, Appl. Phys. Lett. **83**, 5163–5165 (2003).
[22] M. Feneberg, R. A. R. Leute, B. Neuschl, K. Thonke, and M. Bickermann, Phys. Rev. B **82**, 075208 (2010).

© 2012 WILEY-VCH Verlag GmbH & Co. KGaA, Weinheim

[23] G. M. Prinz, M. Feneberg, M. Schirra, R. Sauer, K. Thonke, S. B. Thapa, and F. Scholz, Phys. Status Solidi RRL **2**, 215–217 (2008).

[24] M. Strassburg, J. Senawiratne, N. Dietz, U. Haboeck, A. Hoffmann, V. Noveski, R. Dalmau, R. Schlesser, and Z. Sitar, J. Appl. Phys. **96**, 5870–5876 (2004).

[25] A. R. Goni, H. Siegle, K. Syassen, C. Thomsen, and J. M. Wagner, Phys. Rev. B **6403**, 6 (2001).

[26] W. Shan, T. J. Schmidt, R. J. Hauenstein, J. J. Song, and B. Goldenberg, Appl. Phys. Lett. **66**, 3492–3494 (1995).

[27] H. Siegle, U. Haboeck, A. Hoffmann, and C. Thomsen, Phys. Status Solidi C **0**, 1710–1731 (2003).

© 2012 WILEY-VCH Verlag GmbH & Co. KGaA, Weinheim